Nuclear Mathematical and Computational Sciences: A Century in Review, A Century Anew
Gatlinburg, Tennessee, April 6-11, 2003, on CD-ROM, American Nuclear Society, LaGrange Park, IL (2003)

THE EFFECT OF CORE MODELING APPROACH ON IRIS SHIELDING CALCULATIONS

Zeev Shayer and Ehud Greenspan
Department of Nuclear Engineering
University of California at Berkeley
CA 94720-1730
zshayer@nuc.berkeley.edu; gehud@nuc.berkeley.edu

Bojan Petrovic
Westinghouse Electric Company
Science and Technology Department
1344 Beulah Rd., Pittsburgh, PA 15235-5083
petrovb@westinghouse.com

ABSTRACT

This work examines the effect of the IRIS reactor core modeling on the average and maximum calculated values of the neutron and gamma fluxes reaching the core barrel and the reactor pressure vessel. The IRIS core design considered is for 1000 MWt and fueled with up to 4.95% enriched uranium dioxide. Three core models are considered: the reference model uses XYZ geometry with explicit description of each fuel assembly and fuel pin. The second core model also uses an XYZ geometry but with homogenized fuel assemblies. The third model uses RZ geometry with two concentric homogenized regions. The MCNP-4B2 Monte Carlo code with continuous energy cross sections are used for the calculations. It is found that the RZ model underestimates the maximum neutron flux in the core barrel by up to a factor of 3 to 4. The neutron and gamma fluxes in the RPV have only weak azimuthal dependence; the peak flux exceeds the average by only about 20%. The IRIS reflector/shield attenuates the neutron flux at the RPV by ~10 orders of magnitude.

Key Words: IRIS, Core model, Shield, MCNP

1. INTRODUCTION

IRIS (International Reactor Innovative and Secure) is a modular PWR featuring simplified design and enhanced safety. Each IRIS module is designed to have a 1000 MWt core that is fueled with up to 4.95% enriched uranium dioxide. Detailed information on the IRIS design is provided in references 1 through 4. The purpose of the work summarized in this paper is to quantify the error bounds associated with use of different methods to model the IRIS core for the purpose of calculation of shielding and of the azimuthal flux distribution in the core barrel and reactor pressure vessel (RPV).

The IRIS core parameters used for the present study are those specified in the IRIS-1000 core benchmark #44, revision 2 [5]. The calculations were performed using three different approaches for modeling the core:

- An explicit description of the reactor core, including individual representation of all fuel pins.
- Each fuel assembly is volume homogenized, but the reactor core is still modeled as an ensemble of assemblies arranged in the actual XYZ geometry.
- The core is represented in RZ geometry. It consists of two homogeneous annular regions: the inner one with 4.95 wt% of ^{235}U and with B-10 burnable poison, and the outer one with 2.60 wt% of ^{235}U.

The Monte Carlo code MCNP-4B2 [6] was used for this study. All the calculations were performed with the core loaded with fresh fuel assemblies. This is considered to be a conservative approach since the power shape peaks at the core periphery at the beginning of cycle.

2. DESCRIPTION OF IRIS BENCHMARK #44

The reactor core configuration for this study is based on Ref. 5 revision 2 and is summarized below. A 0.4 cm thick zirconium shroud is added around each fuel assembly. Following are the basic reactor core parameters:

1. The core consists of 89 fuel assemblies arranged as shown in Fig 1.
2. Nominal fuel assemblies (FAs) contain UO_2 with enrichment of 4.95 w/o ^{235}U.
3. Most of peripheral FAs contain UO_2 with a reduced enrichment of 2.6 w/o ^{235}U.
4. Active fuel height is 14 feet, with axially uniform enrichment (either 2.6 or 4.95 w/o ^{235}U). Some FAs have IFBA (a thin layer of ^{10}B coating fuel pellets). IFBA loading is expressed in mg ^{10}B per cm of fuel rod.
5. When IFBA is used, the ^{10}B coating covers the central 365.76 cm (12 ft). In other words, the fuel stack is axially composed of: 30.48 cm (1 ft) of enriched uncoated fuel, 365.76 cm (12 ft) of enriched coated fuel, and 30.48 cm (1 ft) of enriched uncoated fuel.
6. IFBA coating is asymmetric. The lower half (6 feet) has 20% more ^{10}B than the upper half.
7. Figure 1 depicts the core configuration, i.e., the radial and axial fuel enrichment distribution, the radial view shows only the IFBA loading for the upper half. The lower half looks similar, except that IFBA loading is higher.

This core configuration and fuel specifications were used for benchmarking purposes, as well as for this study, since they contain several challenging features; it does not necessarily represent a practical core configuration. Fuel assembly (FA) forms a 15x15 square matrix (Figure 2). Out of 225 unit cells, 204 are fuel cells, the central position is occupied by an instrumentation tube (IT), while the remaining 20 positions contain guide thimbles (GT) for control rods (CR). Unit cell pitch is 1.5042 cm (0.5922”). Fuel assembly is surrounded on each side by a 0.0508 cm (0.020”) water gap; hence, fuel assembly pitch is 22.664 cm (8.923”). GT and IT unit cells are assumed identical in this calculation. Dimensions, temperatures and compositions are provided in Tables I, II and III. The core barrel is made of SS304 and is 5 cm thick, with inner radius of 137.5 cm and outer radius of 142.5 cm. The RPV cladding is also made of SS304 with a thickness of 0.6 cm; the inner and outer cladding radius is 310.5 cm and 311.1 cm, respectively. The RPV is made of low carbon steel with 28.5 cm thickness; the inner and outer RPV radius is 311.1 cm

and 339.6 cm, respectively. The downcomer is 168.0 cm thick. For the purpose of this study we have assumed that it contains 50% volume fraction of SS304 that is mixed uniformly with the water. This is a higher fraction than that considered for practical design. This difference is not expected to change the effects of the approximations in the core modeling.

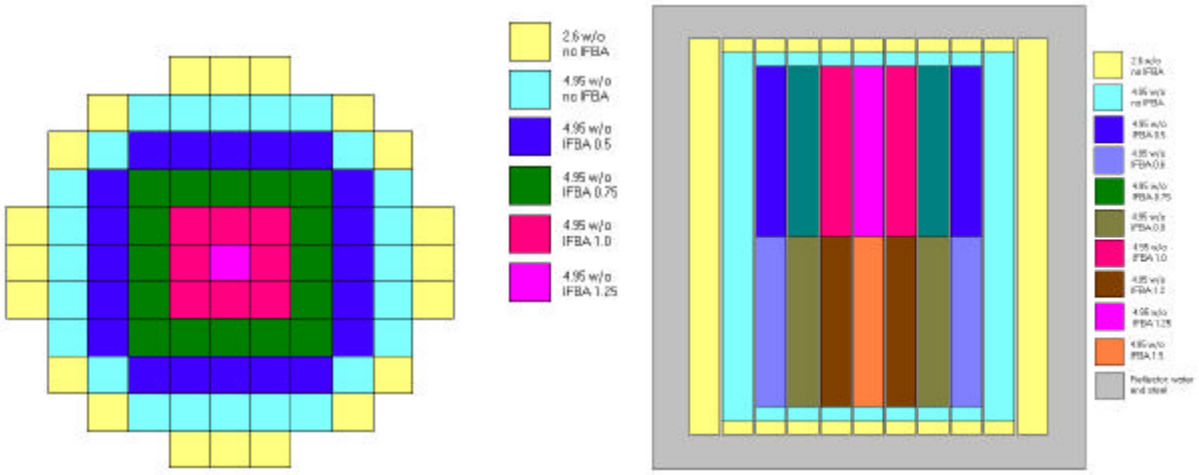

Figure 1. IRIS Benchmark #44: Core configuration vertical and horizontal views including fuel enrichment and IFBA distribution.

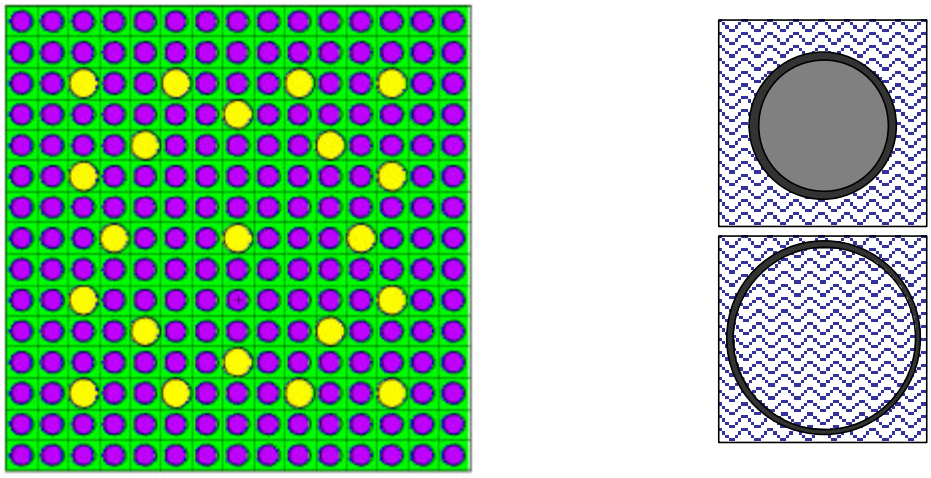

Figure 2. Horizontal cross section of a 15x15 fuel assembly and of its unit-cells.

Table I. Summary of Fuel Unit Cell Geometry

Outer radius of fuel	0.46482 cm (0.183 in)
Outer radius of gap	0.47371 cm (0.1865 in)
Outer radius of Zircaloy-4 clad	0.53721 cm (0.2115 in)
Square lattice pitch	1.50419 cm (0.5922 in)

Table II. Summary of GT and IT Unit Cell Geometry

Inner radius of Zircaloy-4 tube	0.68072 cm (0.268 in)
Outer radius of Zircaloy-4 tube	0.72390 cm (0.285 in)
Square lattice pitch	1.50419 cm (0.5922 in)

Table III. Material and Temperature by Region

Region	Material	Temperature
Moderator	99 $^{v}/_{o}$ water, 1 $^{v}/_{o}$ Zirc-4	584.15 K (311 C, 591.8 F)
Fuel Clad	Zirc-4	616.48 K (343.33 C, 650 F)
GT and IT guide tubes	Zirc-4	T_{mod} (311 C)
Fuel	UO_2	810.93 K (537.78 C, 1000 F)
Reflector	50 $^{v}/_{o}$ water, 50 $^{v}/_{o}$ SS-304	T_{mod} (311 C)

As the calculations are done for beginning-of-life composition, only prompt fission gamma rays and secondary gamma rays from neutron interactions were considered for the gamma source.

3. MCNP METHODOLOGY

All the calculations were done with the MCNP-4B2 Monte Carlo code [6] using ENDF/B-V based point energy cross-section data processed for 300K. Use of ENDF/B-VI cross sections and use of cross-sections processed for the actual reactor operating temperatures will not affect the conclusions from this comparative analysis. MCNP was applied to perform criticality calculations using its eigenvalue mode of solution, and to obtain azimuthal distributions of neutron and gamma fluxes impinging on the core barrel and RPV using an external source mode of solution. The latter calculations assumed a Watt fission spectrum and predetermined fission source distribution across the core. Tallies of the scalar flux were done for azimuthal segments of 10 degree wide across the core barrel or RPV. Only the upper right quarter of the reactor core is used for comparison of the flux tallies. The MCNP results are multiplied by 7.557×10^{19} n/sec to normalize them to a thermal power of 1000 MW.

4. RESULTS

4.1 Eigenvalue

Table IV compares k_{eff} as calculated for the three core models. The reflector thickness is 168.0 cm and is made of 50 $^{v}/_{o}$ SS304 and 50 $^{v}/_{o}$ H_2O. It is concluded that core cylindrization results in a ~2.5% underestimation of k_{eff}. Simple volume homogenization of the core underestimates k_{eff} by ~7%. It should be emphasized, though, that such a volume homogenization is not commonly done for k_{eff} calculations. It is done, however, for shielding analysis.

Table IV. k_{eff} values for IRIS benchmark 44

Case Type	$k_{eff} \pm 2\sigma$
Heterogeneous XYZ	1.26507±0.00038
Homogeneous XYZ	1.17717±0.00006
Homogeneous RZ	1.15254±0.00013

4.2 Azimuthal Distribution of Neutron and Gamma Fluxes

The azimuthal neutron flux distributions were calculated for 3 broad energy groups: "fast flux" covering the energy range above 1 MeV, "resonance flux" covering the energy range between 1 MeV and 0.625 eV, and "thermal flux" covering the energy range below 0.625 eV, as well as for the total flux. The azimuthal gamma flux distributions were calculated for the total gamma flux. The results represent average fluxes over the barrel and RPV thickness and height. The zero degrees in the following figures correspond to the X direction.

4.2.1 Core Barrel

Figures 3 and 4 show the azimuthal distribution of the neutron and gamma fluxes, respectively, in the IRIS core barrel. Both figures pertain to the heterogeneous XYZ core model. The asymmetry in the azimuthal flux distribution is due to inadequate convergence of the fission source spatial distribution in the Monte Carlo calculations; 5000 cycles of 3000 source neutrons per cycle were used. Increasing the number of source neutrons is expected to make the flux distributions more symmetric. The general conclusions, nevertheless, are not expected to vary.

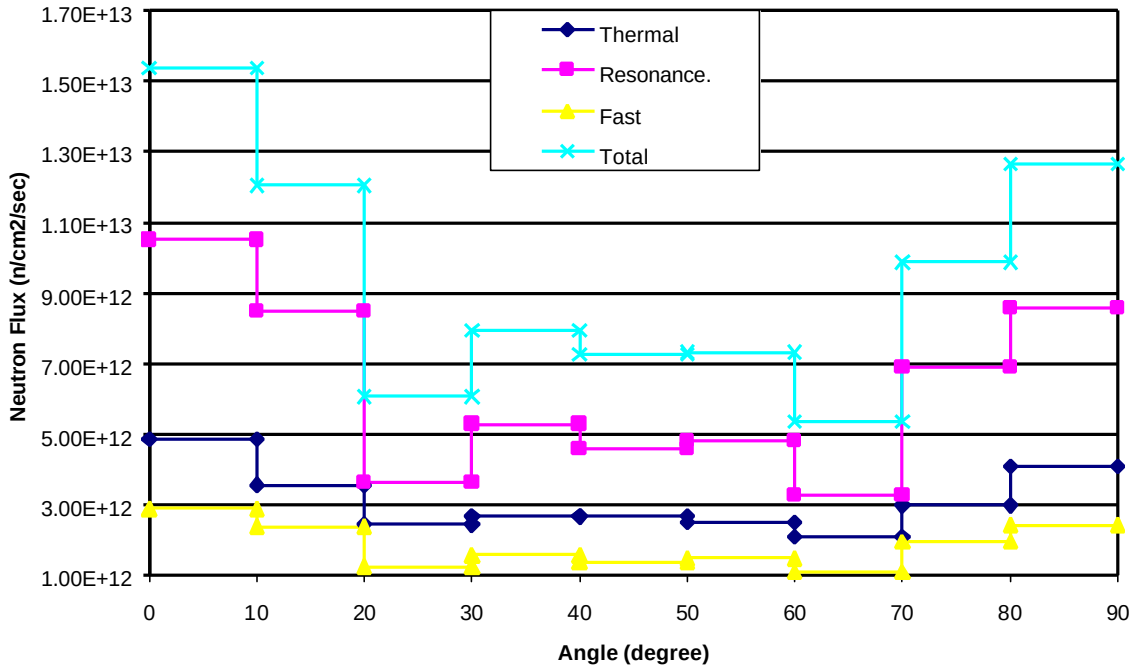

Figure 3. Neutron flux in the IRIS core barrel for various azimuthal angles calculated using the heterogeneous XYZ core model.

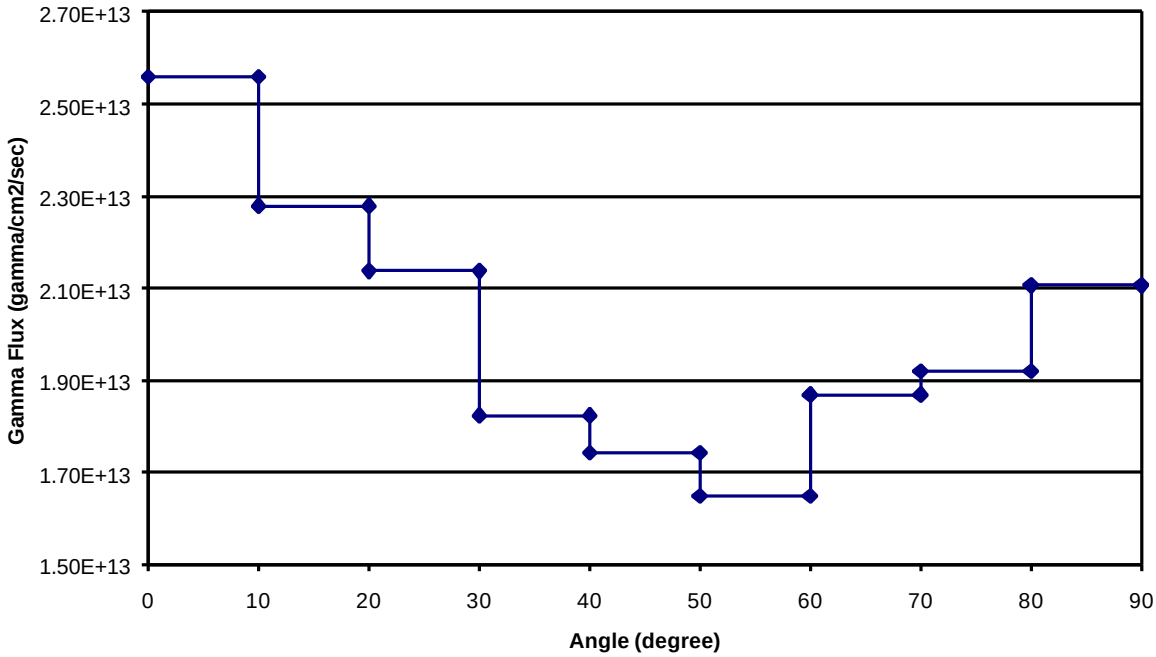

Figure 4. Gamma flux in the IRIS core barrel for various azimuthal angles calculated using the heterogeneous XYZ core model.

Figures 5 through 9 compare the two XYZ core model results for the azimuthal flux distribution whereas Table V compares the corresponding average fluxes in the core barrel.

Table V. Comparison of Average Neutron Fluxes in the Core Barrel Calculated Using Homogeneous and Heterogeneous XYZ Core Models

	Heterogeneous core model			Homogeneous core model			Average homo-to-hetero ratio
	Min	Average	Max	Min	Average	Max	
Fast	1.09E12	1.83E12	2.90E12	1.14E12	2.00E12	3.33E12	1.09
Epi-thermal	3.27E12	6.23E12	1.05E13	3.29E12	6.76E12	1.16E13	1.09
Thermal	2.10E12	3.10E12	4.85E12	2.21E12	3.15E12	5.00E12	1.02
Total	6.46E12	1.12E13	1.83E13	6.64E12	1.19E13	1.99E13	1.06

The relative errors in individual tallies of azimuthal distribution of gamma rays are less than 1%. The relative errors in individual tallies of azimuthal distribution of neutron fluxes are less than 2%. The maximum neutron and gamma fluxes occur at the intervals of 0 to 10 deg and 80 to 90 deg. There is an unexpected tilt of 10% to 20% between the calculated fluxes in these two segments, in spite of the symmetric core configuration. This indicates that the spatial distribution of the fission neutron source has not been fully converged. Nevertheless, the general conclusions on the adequacy of the core representation model are not expected to be affected by this asymmetry. The homogeneous assembly model tends to overestimate the neutron and gamma fluxes by up to ~10%.

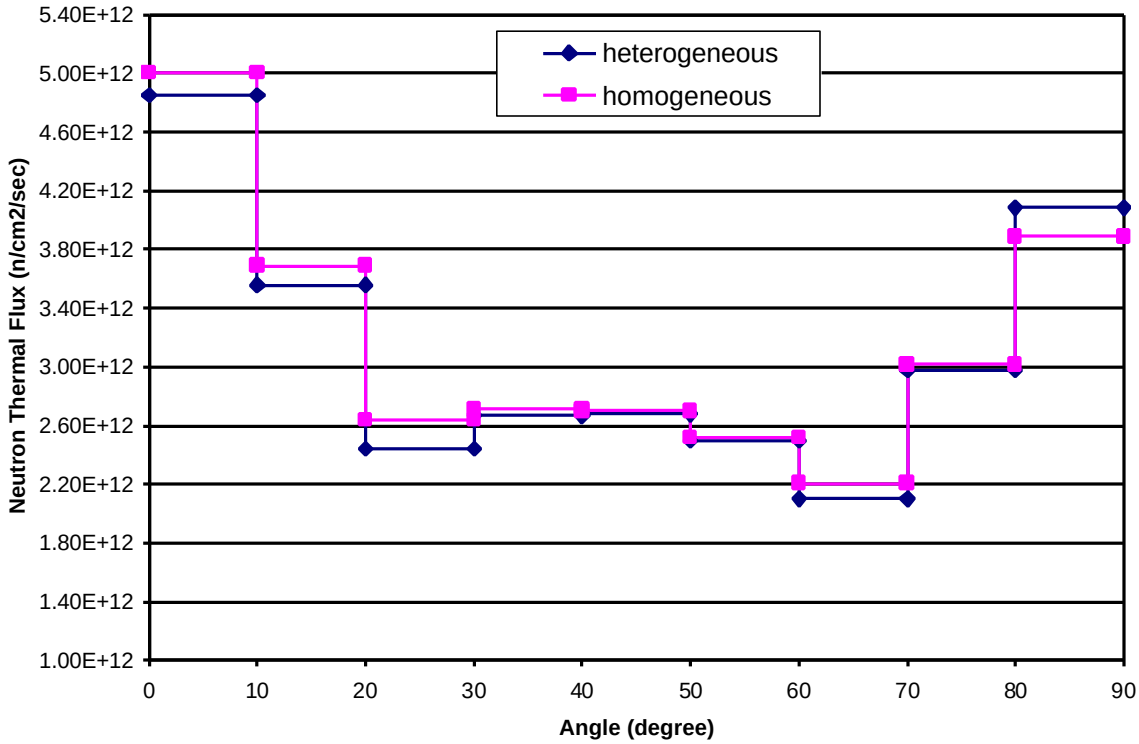

Figure 5. Comparison of neutron thermal fluxes in the IRIS core barrel calculated using the heterogeneous and homogeneous XYZ core models.

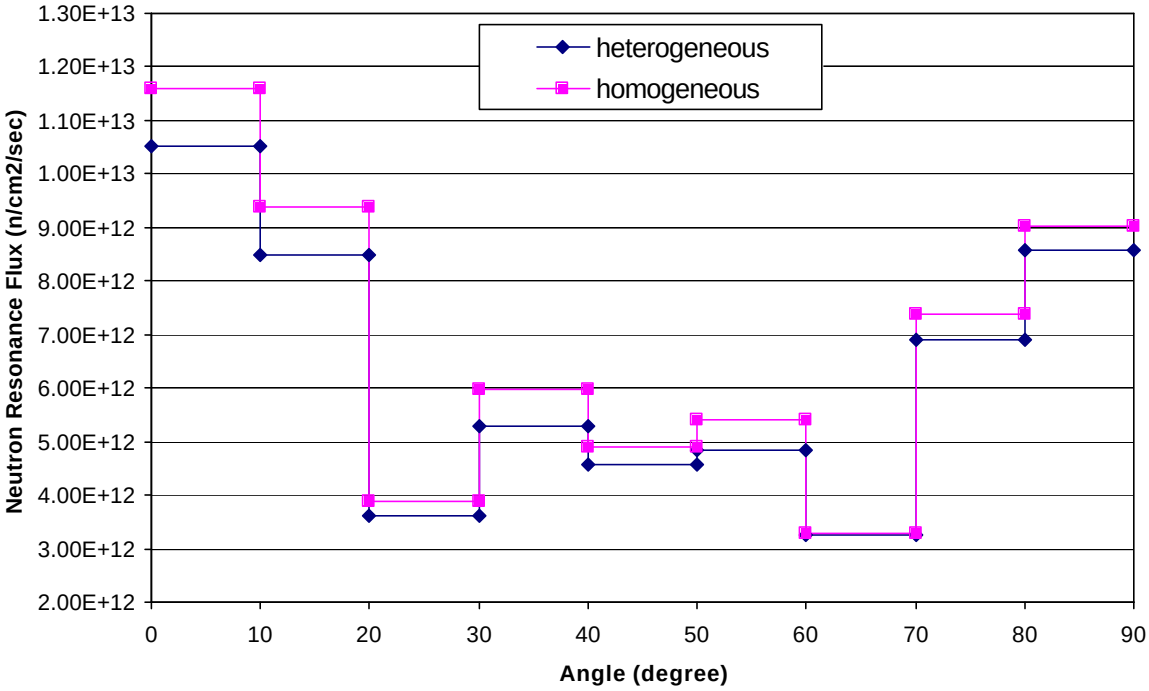

Figure 6. Comparison of resonance neutron fluxes in the IRIS core barrel calculated using heterogeneous and homogeneous XYZ core models.

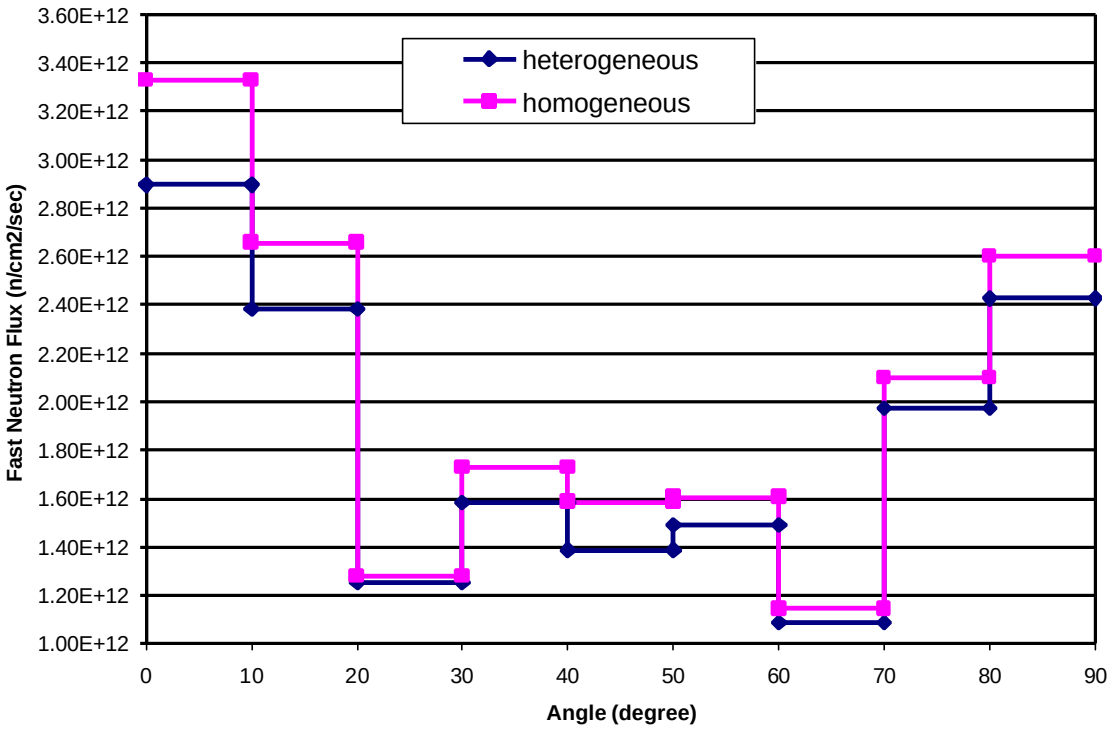

Figure 7. Comparison of fast neutron fluxes in the IRIS core barrel calculated using the heterogeneous and homogeneous XYZ core models.

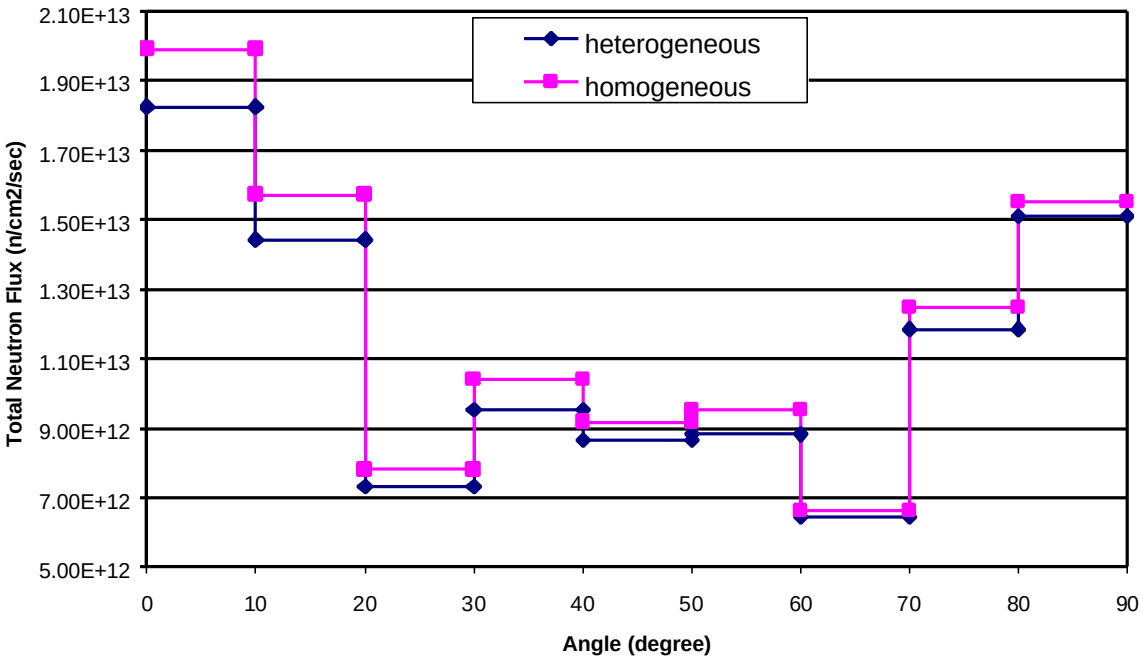

Figure 8. Comparison of total neutron fluxes in the IRIS core barrel calculated using the heterogeneous and homogeneous XYZ core models.

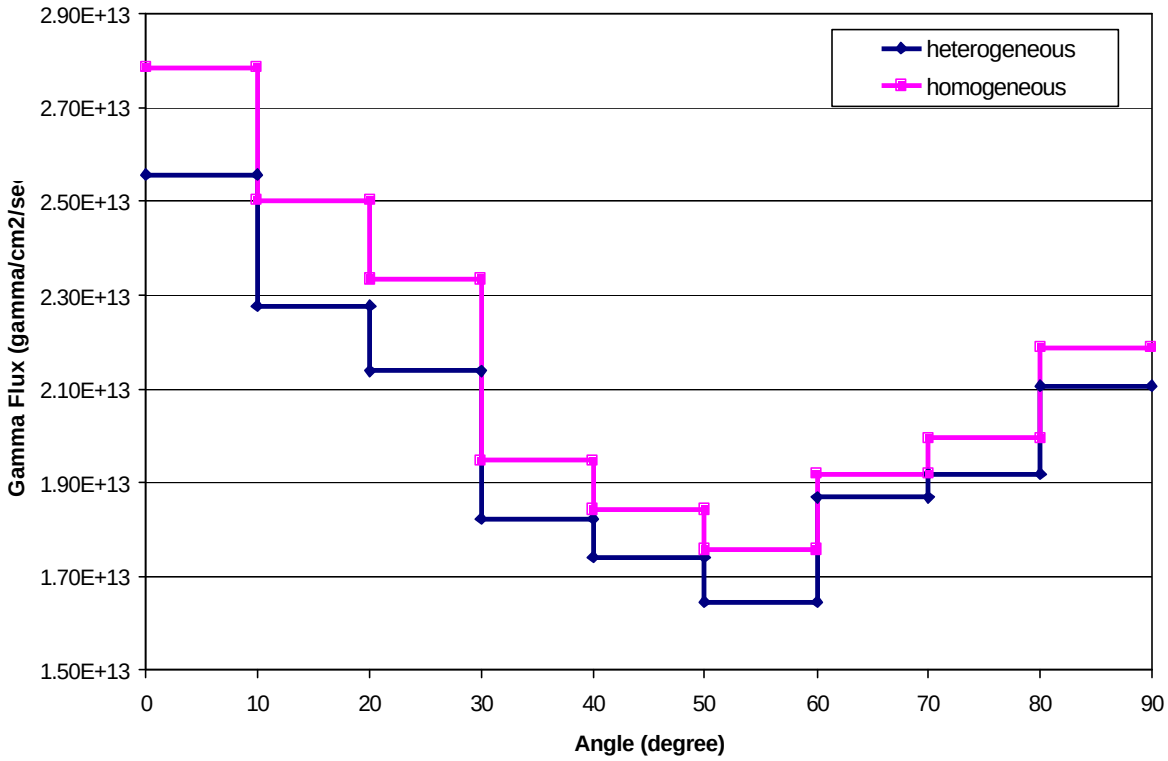

Figure 9. Comparison of gamma fluxes in the IRIS core barrel calculated using the heterogeneous and homogeneous XYZ core models.

Table VI shows the neutron flux comparison between the heterogeneous XYZ core model and the homogeneous RZ one. The average neutron fluxes from the RZ core model are under-estimated by a factor of 2.5 whereas the maximum neutron fluxes are underestimated by a factor of 3 to 4. The same trends are also obtained for the gamma ray distribution over the core barrel.

Table VI. Comparison of Neutron Fluxes in the Core Barrel Calculated Using Heterogeneous XYZ and Homogeneous RZ Core Models

Flux	Heterogeneous XYZ Case			RZ core model	RZ-to-XYZ flux ratio		
	Min	Average	Max		Min	Average	Max
Fast	1.09E12	1.83E12	2.90E12	7.74E11	0.71	0.42	0.27
Epi-thermal	3.27E12	6.23E12	1.05E13	2.35E12	0.72	0.38	0.22
Thermal	2.10E12	3.10E12	4.85E12	1.48E12	0.70	0.48	0.31
Total	6.46E12	1.12E13	1.83E13	4.60E12	0.71	0.41	0.25

4.2.2 Reactor Pressure Vessel (RPV)

Figure 10 shows the azimuthal distribution of the gamma flux in the RPV as calculated using the heterogeneous XYZ core model. The relative error of gamma flux as calculated by MCNP-4B2 in each azimuthal segment is less than 10%. Figure 11 shows the azimuthal distribution of the

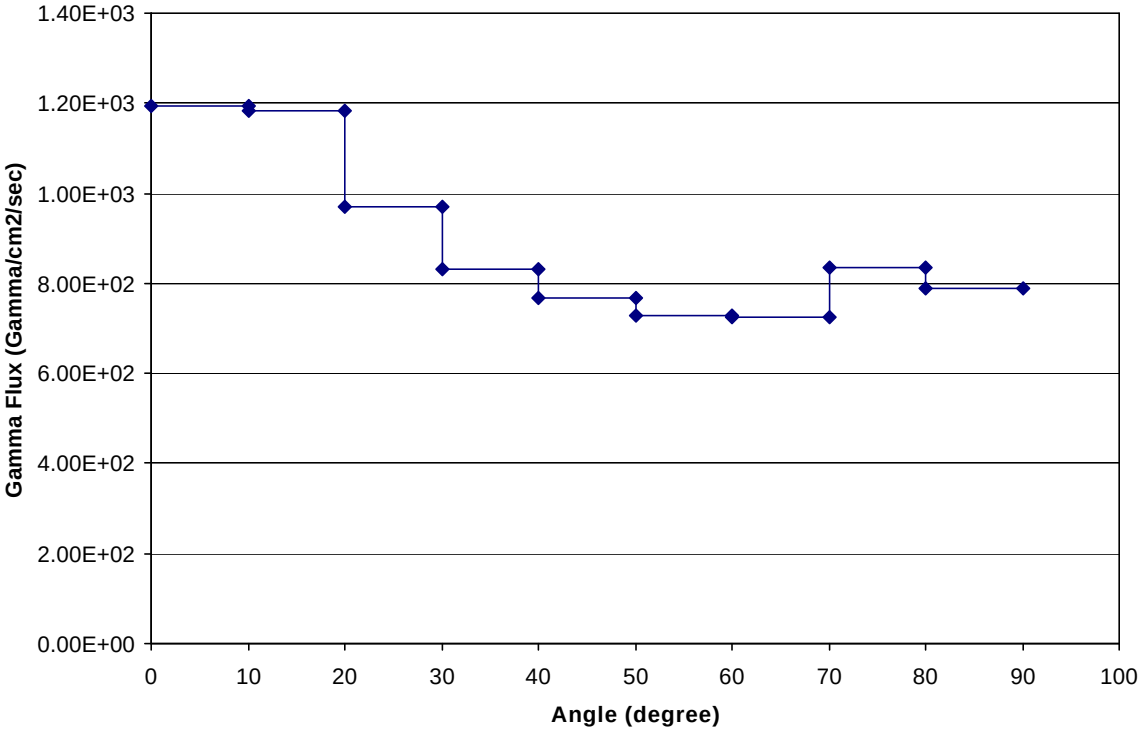

Figure 10. Gamma flux in IRIS reactor PV for various azimuthal angles calculated using the heterogeneous XYZ core model.

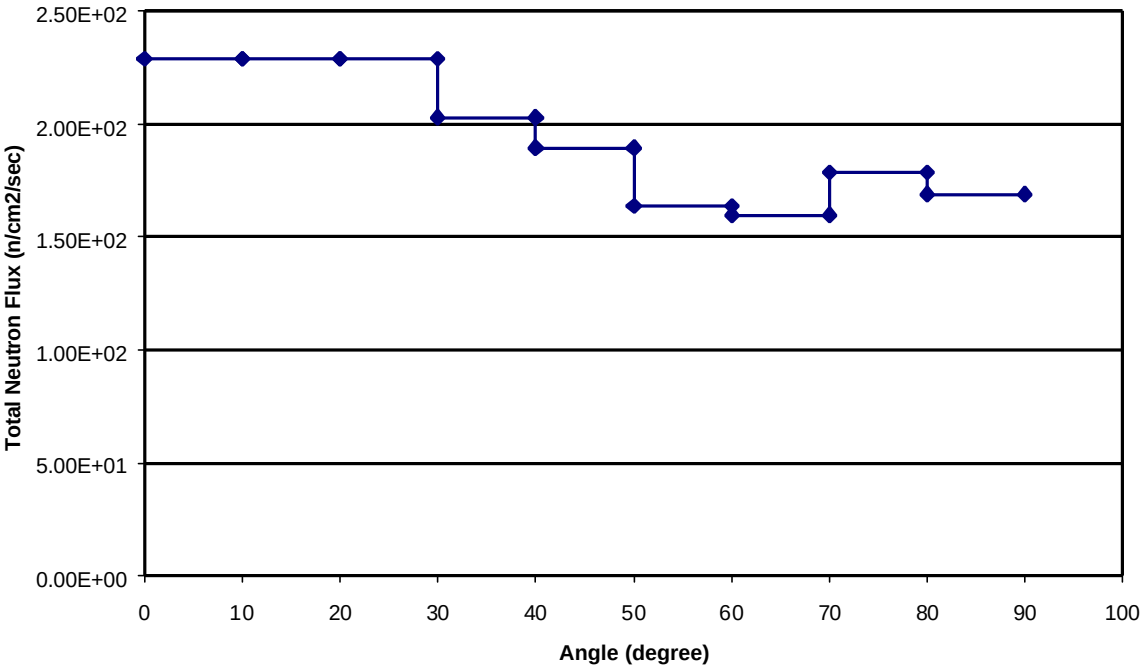

Figure 11. Total neutron flux in IRIS RPV for various azimuthal angles calculated using the heterogeneous XYZ core model.

total neutron flux. The relative error of the total neutron flux in each azimuthal segment is between 10% and 15%. Relative errors in various energy groups were more than 20%; therefore they are not shown in these figures. It can be seen that the neutron and gamma fluxes are smeared out much more evenly over the RPV as compared to over the core barrel; the maximum difference in the azimuthal distribution for gamma and neutron fluxes is less than 50% in the RPV as compared to a factor of three in the core barrel. As the calculation of the fluxes in the RPV took excessive computer time, no calculations were done with the RZ model.

It is also found that the neutron and gamma fluxes in the RPV are ~10 orders of magnitude lower than in the reactor barrel. This attenuation is due to the 168 cm of reflector/shield that is composed of 50% volume fractions of water and SS304. It is the incorporation of the steam generators within the IRIS reactor vessel (above the core level) that creates the wide annular downcomer that offers the possibility to incorporate substantial internal shielding and achieve such a remarkable attenuation. This will lead to very low activation and damage rate in the RPV over the lifetime of the IRIS reactor.

5. CONCLUSIONS

Analysis was performed to evaluate the effects of core modeling approximations on estimated neutron and gamma fluxes in the core barrel and RPV. The main conclusions from this preliminary analysis are:

- Use of volume homogenized fuel assemblies tends to overestimate the fluxes in the core barrel by ~10% for neutrons and by 30% for gammas.
- Use of cylindrical core model underestimates the maximum neutron flux in the core barrel by up to a factor of 3 to 4. The average neutron flux is underestimated by a factor of approximately 2.5.
- The azimuthal distributions of neutron and gamma fluxes are significantly more uniform in the RPV than in the core barrel; the peak flux exceeds the average by only about 20%.
- A reflector/shield consisting of 50% by volume SS304 and 50% water significantly attenuates the neutron and gamma fluxes that reach the pressure vessel – by about 10 orders of magnitude (from ~10^{13} to ~10^{3} for gammas and ~10^{2} for neutrons).
- Due to very low neutron and gamma fluxes that reach the RPV, it is expected that very low activation and damage rates in the RPV will occur over the lifetime of the IRIS reactor.

ACKNOWLEDGEMENTS

The financial support of the IRIS program (NERI Grant DE-FG03-99SF21901) by the US DOE is gratefully acknowledged. Contributions by the IRIS consortium members were invaluable to the progress of the project.

6. REFERENCES

1. M. D. Carelli and B. Petrovic "Next Generation Advanced Reactor", *Nuclear Plant Journal*, May-June 2001, pp. 33-36.
2. M. D. Carelli, L. E. Conway, B. Petrovic, D. V. Paramonov, M. Galvin, N. E. Todreas, C. V. Lombardi, F. Maldari, M. E. Ricotti and L. Cinotti, "IRIS Reactor Conceptual Design," *Intl. Conf. On the Back-End of the Fuel Cycle (Global 2001)*, Paris, France, September 9-13, 2001.
3. M. Carelli, K. Miller, C. Lombardi, N. Todreas, E. Greenspan, H. Ninokata, F. Lopez, L. Cinotti, J. Collado, F. Oriolo, G. Alonso, M. Moraes, R. Boroughs "IRIS: Proceeding Towards the Preliminary Design", *Proc. 10th International Conference on Nuclear Engineering (ICONE-10)*, April 14-18, 2002, Arlington, VA, USA, Paper ICONE10-22497.
4. B. Petrovic, "IRIS Neutronic Analysis and Core Design: Overview & Benchmarks," 5th IRIS Project Meeting, Frederick, MD, April 25-27, 2001; and, B. Petrovic, "IRIS Neutronics and First Core Design: Objectives, Issues, Status," 6th IRIS Project Meeting, Pisa, Italy, October 17-19, 2001.
5. B. Petrovic, "IRIS Neutronics/Core Design Benchmark Problem Specifications – Benchmark 44: Core Depletion Analysis Without Feedback," *Report IRIS-WEC-12 (Rev. 2)*, pp. 30, Westinghouse (January 2002).
6. J.F. Briesmeister, Editor, "MCNP™ – A General Monte Carlo N-Particle Transport Code, Version 4C," LA–13709–M Report, Los Alamos National Laboratory, April 2000.